

# EVALUATION OF QUANTIFICATION TG METHODS FOR CARBONATES IN CARBONATED CEMENT PASTES

Zhenzhen WANG<sup>\*1</sup>, Abudushalamu AILI<sup>\*2</sup>, Go IGARASHI<sup>\*3</sup>, Ippei MARUYAMA<sup>\*4,5</sup>

## ABSTRACT

The study discussed quantification methods of carbonates in cement pastes of natural and accelerated carbonation by TG, combined with XRD-Rietveld analysis. The stepwise method gives a similar carbonate amount to that by Rietveld analysis. The other two methods overestimate the background mass loss and neglect CO<sub>2</sub> released outside the determined temperature range. Furthermore, the lattice parameters of carbonates manifested the reason for the change in carbonate decomposition temperature.

**Keywords:** quantification analysis, calcium carbonates, carbonation, cement paste, TG, XRD

## 1. INTRODUCTION

As the carbon neutrality society develops, the quantification of carbonates in hardened cement-based materials has attracted increasing attention for carbon sinks. However, there are some difficulties in quantifying the carbonate amount in samples with high accuracy due to the complex proportions of building materials, changing carbonation conditions, and different carbonate compositions [1]. Some related ambiguous points need to be discussed.

Generally, the thermogravimetric analysis (TG) and X-ray diffraction analyses (XRD) are the most powerful measurement means to be used widely, despite there are other optional testing means, such as Fourier transform infrared spectroscopy [2], Raman spectroscopy [3], isotope ratio mass spectroscopy [1], CHNS elemental analyzer [1], accelerated mass spectroscopy [4], X-ray imaging [5], gas chromatography [6], and so on. However, given the expensive testing cost and complex preprocessing procedures of samples, other measurement methods are restricted in the promotion to quantify the carbonates in cement-based materials. Therefore, this study investigated and discussed different quantification analysis methods by TG, combined with Rietveld analysis by XRD.

In terms of TG data analysis, three different analysis methods were discussed in the paper as follows, the tangential method, the stepwise method, and the tangent intersection method [7]. Lothenbach et al. [7] compared the quantification results of portlandite (CH) from 430~520 °C by three methods as above, they found although the result of the stepwise method is in accord with the quantification results of XRD, it overestimated content of CH in hardened cement pastes (hcp) by 26% of the actual amount of CH. However, the

tangential method showed a reasonable CH amount in hcp, because it reduces the interference of the background mass loss resulting from the decomposition of amorphous phases and other crystals below 520 °C [7]. Finally, the tangential method is applied widely to quantify the amount of CH in hcp, while it is still disputable to quantify the carbonate amount. In the experiment of Jeong et al, the difference between the carbonate content of TG and the quantification results of XRD can reach 20% by the tangential method [8].

Similar to the tangential method, the stepwise method is also simple to be applied widely. Hong et al [5] quantified the carbonates in the range of 550~950 °C with the stepwise method. Finally, the quantification result of TG is smaller than that of XRD imaging by 13% of total carbonate content in hcp. The quantification error of the stepwise method seems to be smaller than that of the tangential method.

In addition, the decomposition temperature range of carbonates has a vital impact on the error of different methods to quantify the carbonate content by TG. Although Lothenbach et al. [7] mentioned that mass loss of calcium-silica-hydrate gels (C-S-H) mainly occurs at a temperature lower than 600 °C, some CO<sub>2</sub> gases were from the decomposing amorphous calcium carbonate (ACC) at 400~600 °C, but above 600 °C the mass loss primarily due to the decomposition of carbonate crystals. In DTG curves, peaks of carbonates usually depend on cementitious matrix systems, mixing proportion of binders, carbonation conditions, the microstructure of carbonates, and the crystallization degree of carbonates. The corresponding temperature range of the peaks can broaden from 350 °C to 1000 °C [9-12]. While the lowest decomposition temperature of the peak of CH was about 350 °C [12], there is a possibility that the peak of CH overlapped with that of

\*1 Ph.D. student, Graduate School of Environmental Studies, Nagoya University, JCI Student Member

\*2 Assistant Prof., Graduate School of Environmental Studies, Nagoya University, Dr.E., JCI Member

\*3 Associate Prof., Graduate School of Environmental Studies, Nagoya University, Dr.E., JCI Member

\*4 Prof., Graduate School of Environmental Studies, Nagoya University, Dr.E., JCI Member

\*5 Prof., Graduate School of Engineering, the University of Tokyo, Dr.E., JCI Member

carbonates below 600 °C. It is hard to evaluate the carbonate amount in the range of 350~600 °C for deep carbonated samples. Generally, in carbonated hcp, the decarbonization temperature of monocarbonates (Mc), hemicarbonates (Hc), and poorly crystallized calcite is at 550~680 °C, lower than that of well-crystallized calcite at over 720 °C [7,11-13]. Although there is no mass change for partial aragonite and vaterite transformed to stable calcite starting from 400 °C [7,12], the other part decomposed to CO<sub>2</sub> and CaO due to their lattice parameters and lower lattice strain [14,15]. Karunadasa et al investigated the decomposition of calcite by in-suit XRD and found the lattice parameter “c” expands when decomposition temperature increased, but the value of “a” offset negatively [14], conducted the same conclusion as Lucas et al [15]. However, the relationship between lattice parameters and the decomposition temperature of carbonates is still obscure.

Faced with the situation above, this paper not only discussed the comparison among three different TG analysis methods, but also discussed the decomposition temperature range of carbonates by combining XRD measurement. Lattice parameters of carbonates and the carbonate composition were provided by XRD-Rietveld analysis.

## 2. EXPERIMENTAL PROCEDURES

### 2.1 Materials and Specimens

#### (1) Materials

Ordinary Portland cement of N-type from Mitsubishi Material Corporation was mixed with water by the ratio of 1:0.55 to obtain pastes. The mineral and chemical composition of cement are shown in Table 1.

Table 1 Mineral and chemical composition of the OPC cement

Type	N	Chemical composition (%)	
Density	3.16 g/cm <sup>3</sup>	SiO <sub>2</sub>	20.35
Blaine value	3650 g/cm <sup>2</sup>	Al <sub>2</sub> O <sub>3</sub>	5.22
Mineral composition (%)		Fe <sub>2</sub> O <sub>3</sub>	2.78
3CaO·SiO <sub>2</sub>	53.90	CaO	64.71
2CaO·SiO <sub>2</sub>	23.36	MgO	1.16
3CaO·Al <sub>2</sub> O <sub>3</sub>	6.76	SO <sub>3</sub>	2.62
4CaO·Al <sub>2</sub> O <sub>3</sub>	8.37	Na <sub>2</sub> O	0.26
Bassanite	1.70	K <sub>2</sub> O	0.31
Gypsum	0.33	Cl <sup>-</sup>	0.01
CaCO <sub>3</sub>	3.92	Ig.loss	1.88
Total	98.34	Toal	99.30

#### (2) Specimens

For obtaining homogeneous and creamy pastes, the mixing procedures of cement pastes in two steps. Firstly, cement pastes were mixed with deionized water by w/c= 0.3 in a planetary centrifugal mixer (ARE-500) at 1000rpm/min for 1.5min. Then after adding the remaining deionized water to the mixture to confirm the final ratio of total water to cement is 0.55, the pastes continued to be mixed for 1min at 1000 rpm/min. To prevent bleeding, the cement pastes were mixed with a steel spatula every 30 min until the pastes got creamy

and homogenous throughout. While in the accelerated carbonation experiment, the final mixing procedure as above was performed by the Glassic Tube Roller MX-T6-X. Finally, pastes were cast into polypropylene tubes (PP tubes) and vibrated by a vibratory packer (VP-150D) at 2400 vpm for 1 min 30 s. After sealing samples in PP tubes with Aluminum adhesive tapes and parafilm, the PP tubes were preserved, under 20 °C for over 200 days.

### 2.2 Carbonation Conditions

After the hydration age of 200 days, highly hydrated cement pastes were demolded and ground into powder less than 90 μm. Not carbonated powders were prepared under N<sub>2</sub> gases in a glove box. Other powders were then spread uniformly on a clean dish into a layer thickness of 0.2~0.3 mm for carbonation. The fineness of the powders and thin layer guaranteed the homogeneity of the carbonation. Finally, after the carbonation age, samples were collected into PP tubes and sealed by parafilm within an aluminum bag, other than CO<sub>2</sub> absorbents and silica gels, to reduce the carbonation risk of samples. In this study, to check the practicality of quantification methods of TG and XRD analysis, samples from (a) natural carbonation and (b) accelerated carbonation were investigated.

#### (1) Natural carbonation

Table 2 Indoor natural carbonation conditions

Conditions	Max	Min	Average
Temperature (°C)	26.3	9.5	17.7
RH (%)	96.2	18.2	55.6
CO <sub>2</sub> concentration (ppm)	415	359	380

Hcp powdered by the agate mortar was put in an open chamber indoors and exposed to atmospheric CO<sub>2</sub> for 7, 28, and 91 days for natural carbonation. During the carbonation duration, the fluctuation of relative humidity and temperature was recorded by Testo 147H, as shown in Fig .1. The CO<sub>2</sub> concentration was detected by the portable CO<sub>2</sub> sensor periodically. Average, maximum, and minimum value of CO<sub>2</sub> concentration was summarized in Table 2, together with temperature and relative humidity.

#### (2) Accelerated carbonation

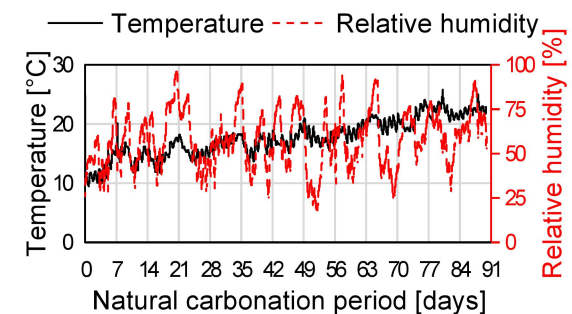


Fig.1 Temperature and relative humidity of the natural carbonation environment.

In the beginning, samples powdered by the ball milling machine were put in a closed plastic box with

the super-saturated solution of NaI to control the RH at 60% for 3 weeks. After that, samples were put into CO<sub>2</sub> incubators with 1% CO<sub>2</sub>, at 20 °C and RH 60%. Samples were carbonated for 0, 1, 3, and 7 days.

### 2.3 Thermogravimetry-Differential thermal analysis (TG-DTA)

Here, natural carbonated hcp powders were equilibrium to RH11% for two weeks, while accelerated carbonated hcp powders were freeze-dried for 48h of a pre-treatment method. The quantification of calcium carbonates in ca 20 mg samples was measured by the thermal gravimetry instrument (TG-DTA 2010 SA-NG21, ASC 7000s, Bruker) under N<sub>2</sub> flow to heat from the ambient temperature to 980 °C at the speed of 10 °C/min, the TG data derived from the different thermal analysis Ver. 4.01. The samples were measured three times per batch of experimental conditions.

Table 3 Temperature range corresponding to decomposition of carbonate phase.

Natural carbonation age (d)	T <sub>1</sub> (°C)	T <sub>2</sub> (°C)	Accelerated carbonation age (d)	T <sub>1</sub> (°C)	T <sub>2</sub> (°C)
0	525	680	0	525	680
7	483	725	1	500	730
28	420	760	3	475	760
91	345	830	7	485	765

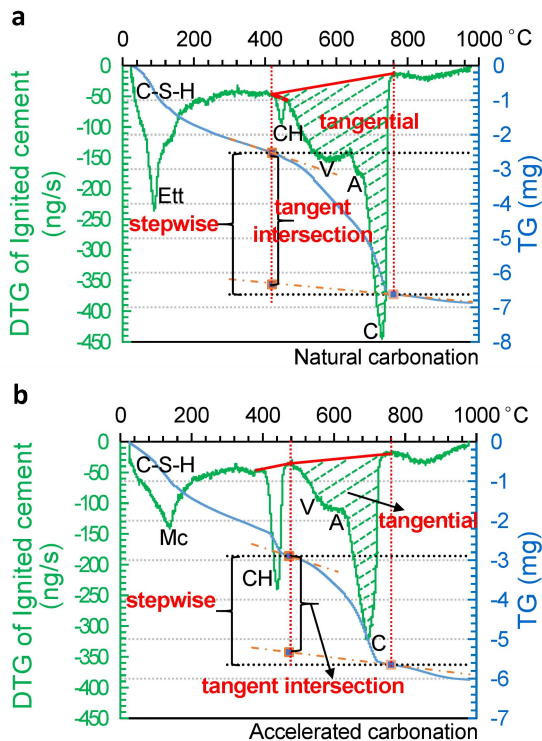


Fig.2 The quantification methods of carbonates in hcp of (a) natural carbonation for 28d; (b) accelerated carbonation for 3d

Carbonate content in hcp was quantified from the mass of released CO<sub>2</sub> due to the carbonate decomposition, whose decomposition temperature

range, T<sub>1</sub>~T<sub>2</sub>, was determined by the peak shape of carbonates in DTG curves and listed in Table 3. Three methods were considered in the range of T<sub>1</sub>~T<sub>2</sub> [7]: 1) stepwise method: the mass loss is equal to the mass of released CO<sub>2</sub> total. 2) tangential method: the mass loss was assumed to include a background mass loss due to H<sub>2</sub>O release from C-S-H and other phases. The background mass loss corresponds to the trapezoidal area, while the CO<sub>2</sub> mass is equal to the area of the green slashed part. 3) tangent intersection method: similar to the tangential method, there was also the background due to the interference of H<sub>2</sub>O. The amount of CO<sub>2</sub> was determined by intersected tangents in TG curve, as shown in Fig .2.

The mass of released CO<sub>2</sub> was marked as  $m_{CO_2}$ . With the molar mass of CO<sub>2</sub> ( $M_{CO_2}$ ) and that of CaCO<sub>3</sub> ( $M_{CaCO_3}$ ), the amount of CaCO<sub>3</sub> in hcp was calculated by Eq. 1:

$$m_{CaCO_3, sample} = m_{CO_2} \frac{M_{CO_2}}{M_{CaCO_3}} \quad (1)$$

### 2.4 X-ray Powder Diffraction (XRD)

As the internal standard reference, 10 wt% of  $\alpha$ -corundum was mixed with hcp powder in an agate mortar under a glove box filled with N<sub>2</sub>.

The phase compositions and hydration degree of hcp specimens were analyzed via X-ray powder diffraction instrument (D2 phaser Bruker 2nd Gen) and Rietveld analysis (TOPAS Ver. 6.0, Bruker AXS). The measurement conditions were as follows: Cu-K $\alpha$  tube with 1.54184 [Å], the tube voltage 30kV, tube current 10.0mA, 2 $\theta$  scan range 5-70 ° by the scan speed of 4.4s/ step with the scan width of 0.02 °. Structural models for the minerals (alite, belite, cubic-C<sub>3</sub>A, and C<sub>4</sub>AF) were taken from an NIST Technical Report. Others for bassanite, gypsum, calcite (C), aragonite (A), vaterite (V), portlandite (CH), ettringite (Ett), mono-carbonate (Mc), hemicarbo-alumination (Hc), hydrogarnet (C<sub>3</sub>AH<sub>6</sub>, Hg), and corundum were taken from the ICSD database. The variation of all phases as above will be analyzed quantitatively. The halo pattern of the amorphous phase was refined as a background function [16]. The samples were measured three times per batch of experimental conditions.

## 3. RESULTS

### 3.1 TG measurement results

Fig .3 shows DTG curves of carbonated hcp. As the carbonate amount increased, the decomposition temperature range (T<sub>1</sub>~T<sub>2</sub>) corresponding to peaks of carbonate crystals became broader. At the same time, the contents of C-S-H, CH, Mc, and Ett gradually decreased. In DTG curves, the peak shape corresponding to both portlandite and carbonates varied significantly. The lower decomposition temperature boundary of the peak of CH increased from 420 °C to 480 °C, while the higher boundary of the peak of calcite increased from 650 °C to 720 °C. In addition, the decomposition temperature range of carbonates became

broader with the increasing carbonation degree. It is probably due to the presence of vaterite and aragonite, which made the peak wider and blunt, quite different from the typical sharp peak of calcite.

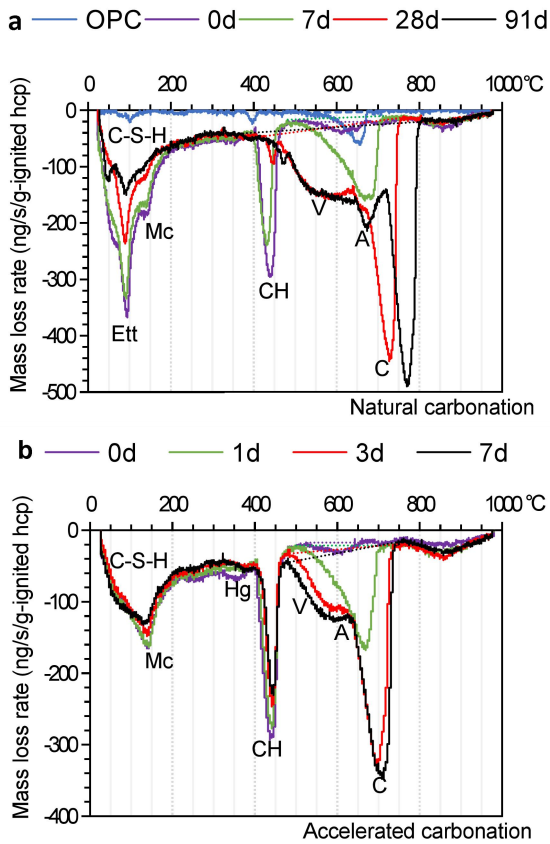


Fig.3 DTG curves of hcp, (a) natural carbonation; (b) accelerated carbonation. The dotted line shows the temperature range of carbonate decomposition.

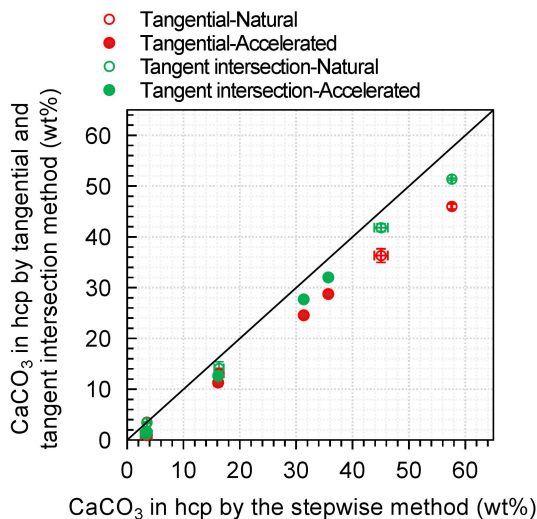
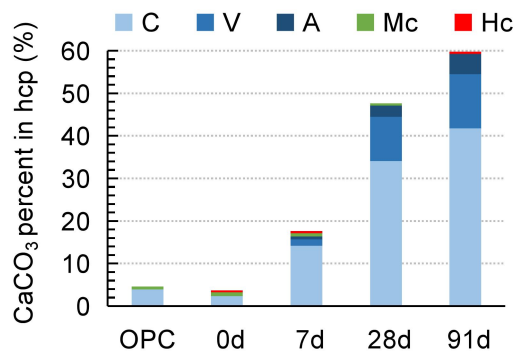


Fig.4  $\text{CaCO}_3$  amount in hcp from natural carbonation and accelerated carbonation, based on different quantification methods of  $\text{CaCO}_3$  (here the error bar of the X-axis indicated the error of the stepwise method, while the error bar of the Y-axis manifested the error of the tangential method and tangent intersection method respectively).

Fig. 4 compares the carbonate amount quantified by the stepwise method with that by the tangent method and the tangent intersection method. As expected from the assumption of each method, the carbonate amount was highest in the stepwise method and the smallest in the tangential method, which is also consistent with the conclusion of Lethenbach et al. [7]. The difference between the stepwise method and the other two methods increased with the increase of carbonate amount. The maximum gap of the quantified carbonate content in hcp between the stepwise method and that of the tangential method was 11.2% for the naturally carbonated sample of 91 days. At the same time, for the tangent intersection method, the maximum difference with the stepwise method was 6.2%. The corresponding maximum gaps between the stepwise method and the other two methods in the hcp of accelerated carbonation were 6.9% and 3.7%, respectively.

### 3.2 XRD measurement results

#### a-Natural carbonation



#### b-Accelerated carbonation

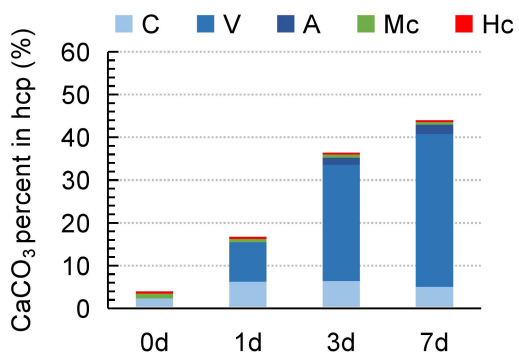


Fig.5 Carbonate amount (%) in hcp from (a) natural carbonation and (b) accelerated carbonation, Hc and Mc have been calculated as the content of equivalent  $\text{CaCO}_3$ .

Fig .5(a) shows the content of calcite is higher than vaterite, followed by aragonite. In Fig .5(b) the vaterite was the dominant carbonate, instead of calcite which is higher than the amount of aragonite. Apparently, the carbonate composition of hcp in accelerated carbonation is different from that of natural carbonation. In addition, for calcite and vaterite, the c of the lattice parameter increased slightly, but the a of

the lattice decreased when the carbonation degree increased, as shown in Table 4. In addition, Table 4 indicated lattice parameters of carbonate crystals changed with the increasing carbonate amount, 'a' of calcite increased with the decrease of the 'c', while the lattice parameters of vaterite shows the contrary trend with calcite.

Table 4 Lattice parameters of calcite and vaterite (Å)

Carbonates	calcite		vaterite		
	a	c	a	c	
Carbonated hcp					
Natural	7	4.9945	17.0831	4.1175	8.5149
carbonation	28	4.9912	17.0945	4.1243	8.4964
age (d)	91	4.9905	17.1000	4.1279	8.4838
Accelerated	1	4.9960	17.0569	4.1179	8.5043
carbonation	3	4.9939	17.0706	4.1233	8.4928
age (d)	7	4.9918	17.0781	4.1246	8.4829

#### 4. DISCUSSION

Different from the stepwise method, the tangential method and the tangent intersection method subtract the assumed background mass loss from the total mass loss in the range of  $T_1 \sim T_2$ . As shown in Fig .2, the assumed background mass loss in the tangent intersection method is only a portion of the trapeze of the background in the tangential method. Hence, the assumed background in the tangent intersection method is smaller than that in the tangential method.

Among the three methods as above, the results of the stepwise method agree best with the results of the XRD-Rietveld analysis. As shown in Fig .6, the  $\text{CaCO}_3$  amount quantified by the stepwise method is equal to or slightly lower than that of XRD. However, the tangential method and tangent intersection method underestimate  $\text{CaCO}_3$  due to two possible reasons: 1) overestimation of the background due to  $\text{H}_2\text{O}$  release; 2)  $\text{CO}_2$  release may occur outside the determinant temperature range.

The degradation of C-S-H and other phases with the carbonation progress may explain the first reason. At 200~400 °C, the mass loss rate due to  $\text{H}_2\text{O}$  release from C-S-H and other phases, as shown in Fig .2, decreased as the carbonation age. The decrease of the background mass loss can be expected in the temperature range of carbonate decomposition. In other studies, referring to the  $\text{H}_2\text{O}$  signal curves, the mass loss rate of  $\text{H}_2\text{O}$  decreased after the decomposition of portlandite [7,11]. Apparently, by the tangential method and tangent intersection method, the background mass loss shows the contrast cases in hcp of (a) natural carbonation for 28 days and 91 days in Fig .3. Based on the different shapes of DTG curves, we infer that the tangential and tangent intersection method was probably reasonable for slightly carbonated samples but may cause the overestimated background mass loss for highly carbonated samples.

In terms of the second reason, as shown in other studies [11,17], the  $\text{CO}_2$  signal was still detected outside the confirmed temperature range of carbonate decomposition. Particularly above 700 °C, the shape of

DTG curves is mainly based on the  $\text{CO}_2$  signal rather than the  $\text{H}_2\text{O}$  signal [11,17]. More importantly, in Fig. 3, as shown in DTG curves of highly carbonated hcp at the carbonation, the peak of carbonate decomposition joined with that of CH, rather than separated by a flat platform as non-carbonated samples, it manifested that the peak of carbonates overlapped with other phases releasing  $\text{H}_2\text{O}$ , outside the range of  $T_1 \sim T_2$ , partial  $\text{CO}_2$  released from decomposing carbonates. As a result, the quantification results of the tangential method and those of the tangent intersection method were undervalued further. Although the stepwise overestimated the carbonate content in the determined decomposition temperature range of carbonates, the error is limited, especially for highly carbonated samples. In fact, it compensated for the neglected  $\text{CO}_2$  outside the range of  $T_1 \sim T_2$ . The comparison of the quantification results between the stepwise method and the Rietveld analysis also supported the above points. Combined with Fig .6, the quantification result of the stepwise method is consistent with the analysis results of the XRD. The average error was only 2%. Therefore, the stepwise method is the most reasonable method among the three methods when compared with the XRD-Rietveld analysis.

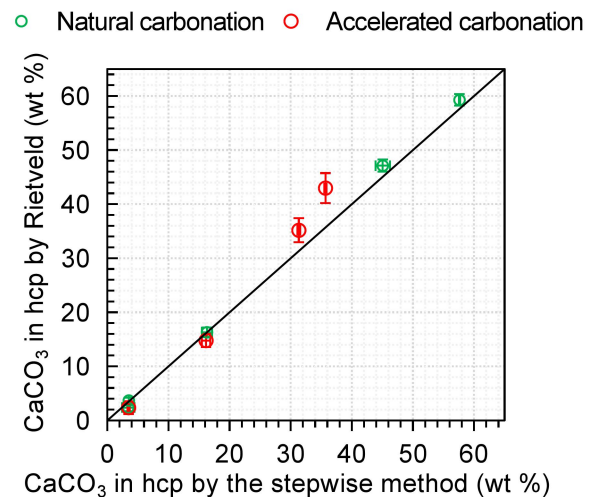


Fig.6 The comparison of the carbonate amount in carbonated samples by XRD-Rietveld analysis method and stepwise method of TG (here the error bar of the X-axis indicated the error of the stepwise method, while the error bar of the Y-axis manifested the error of the Rietveld analysis).

The decomposition temperature range of carbonates directly influenced the accuracy of the quantification results of carbonate content in hcp. Generally, it was confirmed by referring to the peak shape and position in DTG curves. But for highly carbonated hcp, the content of CH also needed to be considered. For example, in hcp naturally carbonated for 28 days and 91 days, when the CH amount decreased to about 1%,  $T_1$  decreased to 350 °C. In addition, although the dominant carbonate crystal has a slight influence on the range of  $T_1 \sim T_2$ , the  $T_1$  decreased as the increase of the content of vaterite, aragonite, and

poorly crystallized calcite, but  $T_2$  depended on the total carbonate amount, as shown in Fig. 5. On the other hand, as shown in Table 4, the 'a' decreased while 'c' increased when the total carbonate amount increased. But the lattice parameters of vaterite showed a contrary variation trend. It may reveal the reason for the broader decomposition range of carbonates in hcp with a higher carbonate degree.

## 5. CONCLUSIONS

For evaluation of carbonates in cement pastes which are carbonated under similar conditions of this study, the following conclusions were drawn:

- (1) For TG measurement, the stepwise method is more reasonable than the tangential method and tangent intersection method, which is the best to agree with the XRD-Rietveld analysis results.
- (2) The tangential method and the tangent intersection method overestimated the background mass loss of  $H_2O$  due to the decomposition of C-S-H and other phases.
- (3) The lattice parameters of calcite and vaterite changed as the amount of carbonates, which could be one of the reasons for the changing decomposition temperature range of carbonates.

## ACKNOWLEDGEMENT

The authors acknowledge the support of the New Energy and Industrial Technology Development Organization (NEDO) for the project, JPNP21023.

## REFERENCES

- [1] Ipei Maruyama, Yoshihiro Asahra, Masayo Minami and Hidekazu Yoshida., "Evaluation of carbonation process in concrete with an analysis of carbon isotopes," *Cement Science and Concrete Technology*, Vol.64, No.1, pp.139-146, 2010.
- [2] Trevor L. Hughes, Claire M. Methven, Timothy G.J. Jones, Sarah E. Pelham, Philip Fletcher, Christopher Hall, "Determining cement composition by Fourier transform infrared spectroscopy," *Advanced Cement Based Materials*, Vol.2, Issue 3,1995, pp.91-104.
- [3] John Bensted., "Raman spectral studies of carbonation phenomena," *Cement and Concrete Research*, Vol.7, No.2, 1977, pp.161-164.
- [4] Tsuyoshi Tanaka, Masayo Minami, Hidekazu Yoshida, Shizuo Yoshida., "14C abundances: An index for weathering of concrete construction", 名古屋大学加速器質量分析計業績報告書, XIX, 2008.03, pp.65-72.
- [5] Shuxian Hong, Rongrong Jiang, Fan Zheng, Shengxin Fan, Biqin Dong., "Quantitative characterization of carbonation of cement-based materials using X-ray imaging", *Cement and Concrete Composites*, Vol.134, 2022, 104794.
- [6] Anna Maria Beccaria, Gildo Poggi, Gianrico Castello., "Gas chromatographic determination of carbonates in the corrosion products of metals", *Journal of Chromatography A*, Vol.395, 1987, pp.641-647.
- [7] Barbara Lothenbach, Paweł T. Durdziński, Klaartje De Weerd., "Thermogravimetric analysis", *A Practical Guide to Microstructural Analysis of Cementitious Materials*, 1st Edition, 2016, CRC Press, p.36.
- [8] Jena Jeong, Abel Shiferaw Alemu, Solmoi Park, Hyo Kyoung Lee, Gebremicael Liyew, Hamidréza Ramézani, Vagelis G. Papadakis, Hyeong-Ki Kim, "Phase profiling of carbonated cement paste: Quantitative X-ray diffraction analysis and numerical modeling, *Case Studies in Construction Materials*, Vol 16, 2022, e00890.
- [9] Goodbrake, C.J., Young, J.F., Berger, R.L., "Reaction of Beta-Dicalcium silicate and tricalcium silicate with carbon dioxide and water vapor", Vol 62, No. 3-4, 1979, pp.168-171.
- [10] Stepkowska, E.T., Aviles, M.A., Blanes, J.M., Perez-Rodriguez, J. L., "Gradual transformation of  $Ca(OH)_2$  into  $CaCO_3$  on cement hydration", *J Therm Anal Calorim*, Vol 87, 2007, pp.189-198.
- [11] M. Thiery, G. Villain, P. Dangla, G. Platret., "Investigation of the carbonation front shape on cementitious materials: Effects of the chemical kinetics", *Cement and Concrete Research*, Vol 37, Issue 7, 2007, pp.1047-1058.
- [12] Yongqiang Li, Tangwei Mi, Wei Liu, Zhijun Dong, Biqin Dong, Luping Tang, Feng Xing, "Chemical and mineralogical characteristics of carbonated and uncarbonated cement pastes subjected to high temperatures", *Composites Part B: Engineering*, Vol 216, 2021, p.108861.
- [13] Zhenjun Tu, Ming-zhi Guo, Chi Sun Poon, Caijun Shi., "Effects of limestone powder on  $CaCO_3$  precipitation in  $CO_2$  cured cement pastes", *Cement and Concrete Composites*, Vol 72, 2016, pp.9-16.
- [14] Kohobhange S.P. Karunadasa, C.H. Manoratne, H.M.T.G.A. Pitawala, R.M.G. Rajapakse, "Thermal decomposition of calcium carbonate (calcite polymorph) as examined by in-situ high-temperature X-ray powder diffraction", *Journal of Physics and Chemistry of Solids*, Vol 134, 2019, pp.21-28.
- [15] Lucas A, Mouallem-Bahout M, Carel C, et al., "Thermal expansion of synthetic aragonite condensed review of elastic properties", *Journal of Solid State Chemistry*, Vol 146, No.1, 1999, pp.73-78.
- [16] Maruyama, I. and Igarashi, G., "Cement reaction and resultant physical properties of cement paste", *Journal of Advanced Concrete Technology*, Vol 12 (6), 2014, pp.200-213.
- [17] I. Maruyama, S. Ishikawa, J. Yasukouchi, S. Sawada, R. Kurihara, M. Takizawa, O. Kontani, Impact of gamma-ray irradiation on hardened white Portland cement pastes exposed to atmosphere, *Cem. Concr. Res.*, Vol 108, 2018, pp. 59-71.